IOSR Journal of Applied Geology and Geophysics (IOSR-JAGG)
e-ISSN: 2321–0990, p-ISSN: 2321–0982. Volume 14, Issue 4 Ser. 1 (July – August 2026), PP 01-13
www.iosrjournals.org

Lateral Variations In Rock Properties Revealed By Acoustic Impedance Inversion: A Case Study Of The Early Palaeogene Heimdal Formation, Northern North Sea

[1]M. Bello, [2]A. M. Kaura, [1]A. Salihu
[1]*Department of Physics, Abubakar Tafawa Balewa University, Bauchi – Nigeria*
[2]*Department of Geology, Federal University Lafiya, Nassarawa State – Nigeria*

Abstract
*This study applies post-stack acoustic impedance inversion to investigate the lateral variability of reservoir properties within the Paleogene Heimdal Formation in the northern North Sea. The analysis utilised 3D migrated partial stack seismic data, 2D CDP gathers, and petrophysical data from five wells penetrating the Heimdal Formation. Well-log derived acoustic impedance models were integrated with seismic data to generate acoustic impedance, velocity and porosity volumes. The inversion results showed that the acoustic impedance values varies from approximately 2000 to 5700 m/s*g/cm³ indicating significant spatial heterogeneity within the reservoir. The relativity low acoustic impedance values suggest that the sandstones are poorly consolidated and moderately compacted. Predicted porosity values vary between 25% and 40 % indicating very good to excellent reservoir quality across much of the study area. The inversion results further reveal marked lateral variations in acoustic impedance and porosity that reflects changes in lithofacies and the complex distribution of turbidite channel sands. Comparison between inversion-derived porosity and well-log porosity at the control well yielded a correlation coefficient of 68 % demonstrating a satisfactory predictive capability of the inversion workflow.*

Keywords: *Acoustic impedance inversion, Porosity prediction, Heimdal Formation, Paleogene, Seismic inversion, Northern North Sea*

Date of Submission: 24-06-2026 Date of Acceptance: 04-07-2026

I. Introduction

Accurate characterization of subsurface reservoirs remains a fundamental objective in petroleum exploration and development because it directly influences hydrocarbon prospect evaluation, reserve estimation, and field development planning. Conventional seismic interpretation provides valuable structural and stratigraphic information; however, it is often inadequate for detailed prediction of reservoir properties such as lithology, porosity, and fluid distribution. Quantitative seismic interpretation techniques, particularly acoustic impedance inversion, have therefore become essential tools for reducing exploration uncertainty and improving reservoir characterization.

This study applies post-stack acoustic impedance inversion to characterize the lateral distribution of reservoir properties within the Heimdal Formation. The objectives are to (i) estimate the acoustic impedance distribution of the reservoir, (ii) predict porosity away from well locations, (iii) evaluate lateral variations in reservoir quality, and (iv) assess the effectiveness of acoustic impedance inversion for reservoir characterization in complex Paleogene turbidite systems of the northern North Sea.

II. Geology Of The Study Area

Paleocene turbidite sands

Paleocene strata are widely distributed and provide one of the most important hydrocarbon accumulations throughout the North Sea Basin (Figure 1). The preserved Paleocene strata in the North Sea Basin comprise siliciclastic sediments with minor amounts of volcanoclastic rocks, tuff, coal, marls and reworked carbonate sediments (Ahmadi *et al.,* 2003). The great volumes of the siliciclastic sediments were primarily sourced from the Scotland-Shetland hinterland (Jordt *et al*., 1993). An important reservoir in the Paleocene strata, which this research work focuses on, is the Heimdal Formation sandstone. The Heimdal sandstone is a late Paleocene turbidite sands characterised by complex thin sands distribution embedded in relatively pure shales (Avseth *et al*., 2005).

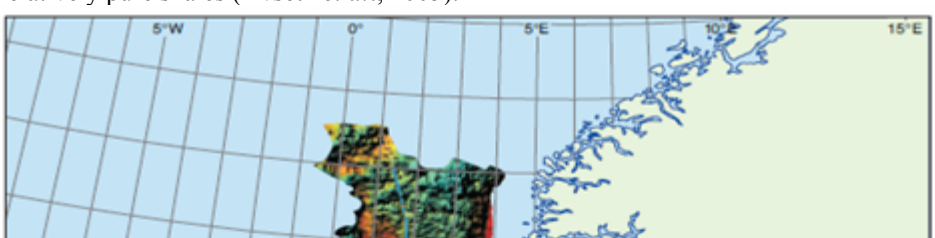

Figure 1. Paleocene distribution in the North Sea. The map shows the thickness of Paleocene strata throughout the North Sea Basin. The thickness data are presented as colour shaded-relief image. The areas of maximum thickness are adjacent to the Shetland platform and the Norwegian landmass. The Halibut Horst was a prominent high throughout the Paleocene times. Precise limits of the Paleocene are not shown. (Ahmadi et al., 2003)

Stratigraphy

The Paleocene and earliest Eocene strata in the North Sea record a second order regression and transgression (Haq *et al*., 1988). Cycles of regressive/transgressive, regardless of order, are characterised by the input of sand into various parts of the basin during the regressions and the confinement of sands deposition along basin margins during transgressions. Individual cycles can exhibit a spectrum of depositional environments that range from shore zone or coastal-deltaic to deep water (Neal, 1996).

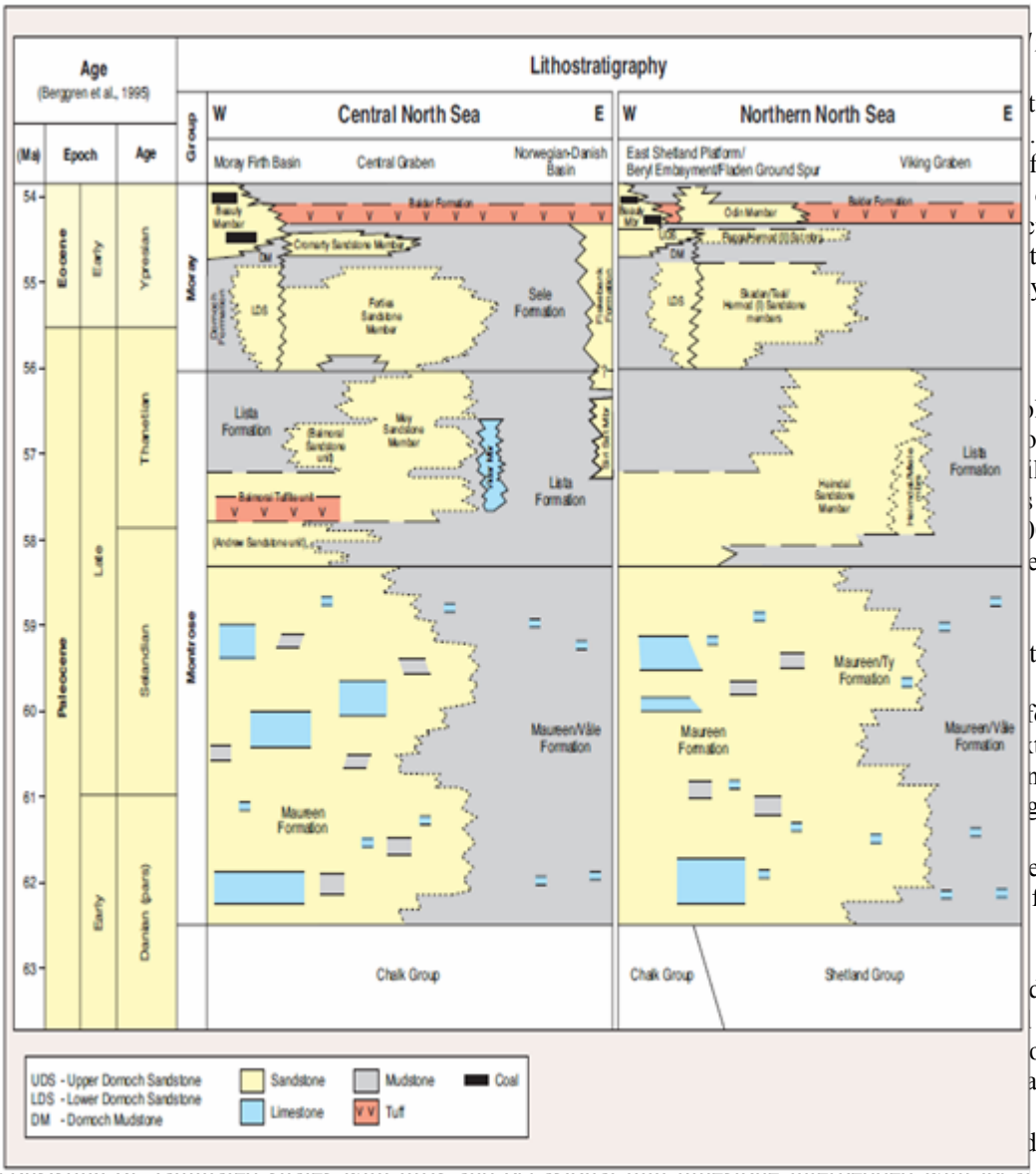

992)

tion (Figure 2), . They form an formally define of the Ekofisk cts fundamental th Sea range in y 1000m in the

lex thin sands ort indicates the lty shale, clean at a measured 000). Individual ed by Heimdal

the central and for Paleocene for oil and gas taposition with ndreds or even gration remains

es. Channelling form excellent 17 to 33% and

d gas, laterally walker, 1993). ow-relief, four- ave also proven

limentary units consisting of: laminated shales with tuffs and occasional thin limestone interbedded with local sandstone that may be massive; overlying fissile and commonly laminated mudstones and sandstones (Knox and Holloway, 1992). The laminated mudstones are underlain by complex thin sands distribution embedded in relatively pure shales (Avseth *et al*., 2000); underneath the interbedded shale-sandstones lay laminated silty shales which are further underlain by pure shales (Whyatt and Rhodes, 1991). The geological setting depicts a complex turbidite sand distribution where assessment of the Paleocene sands based on conventional seismic and well log stratigraphic analysis may be very uncertain in these depositional settings.

Previous geophysical work

Tiekuro et al. (2024) applied Post Stack AI Inversion to predict lateral rock physical properties in Eti-field Offshore Niger delta. The study was able to delineate lateral and vertical alternations in subsurface rock properties which is attributed to differences in lithofacies within the reservoir interval,

Eissa *et al*. (2009) presented a detailed study of thin, porous, gas- saturated sandstone packages in the onshore Guajira Basin of northern Columbia. The sandstone packages are similar to the Heimdal sandstone in terms of complexity and geometry. The study includes acoustic impedance inversion, fluid substitution, and AVO modelling/analysis. The study successfully predicts the thin sandstone reservoirs as heterogeneous in terms of thickness, rock properties and areal distribution and suggested that better imaging of the thin sandstones can be best achieved either by acquiring new seismic data using new technology with better frequency content or by reprocessing existing seismic data for frequency enhancement.

A study by Avseth *et al*. (2009) utilises the application of contact cement model concept to study two clean sandstone intervals, both representing the Palaeocene age Heimdal Formation in the North Sea. Both intervals are oil-filled reservoir sands of commercial interest. The rocks were diagnosed using well log measurements and rock physics theory. It was assumed that if in the velocity-porosity plane of a data point falls close to a theoretical line, the internal structure of the rock would be similar to the idealized structure used in the model. It was found from such diagnostic approach that one interval is composed of unconsolidated sand, while the other interval is composed of cemented high-porosity sand. By studying the seismic signatures of these two different types of clean sands log-based diagnostic was upscale to seismic scale.

Seirra *et al.,* (2009) conducted a study to evaluate the possibility for seismic to discriminate lithology and fluids through attributes derived by elastic inversion in a new prospect down dip and south of Main Saldado Field, Trinidad and Tobago. The Formation studied is also similar to Heimdal Formation in terms of lithology and geometry. The results were integrated with amplitude maps, well information, and structural stratigraphy. They concluded that integrated interpretation of the 3-D seismic volume and well log data delineated several thin discrete stratigraphic features of Miocene age which are potential reservoirs; all techniques applied in the study-including acoustic impedance and elastic impedance, rock physics, and spectral decomposition-show the feasibility that the sands could have acoustic and elastic impedances contrast although the seismic data do not have good resolution. In spite of this the, it was possible to recognise the main geobodies.

To understand how the type of sand (unconsolidated versus cemented) affects the seismic response, Avseth *et al*., (1998) analysed CDP gathers at different well locations where horizons were picked at the top of the Heimdal formation; by using a 30 Hz zero-phase Ricker wavelet synthetic CDP gathers for different wells were produced and a reflectivity series were derived. Both the real and synthetic gathers show reflectivity increasingly negative with increasing offset at the picked horizon. For one well, the reflectivity was plotted versus offset (angle), together with the theoretical Zoeppritz line. The synthetic response appears to be very close to the real data which means that it can be relied on well-log-based rock diagnostic to predict seismic response. This offset-dependent reflectivity analysis shows that clean sands of the same formation, similar porosity, and with comparable oil saturation produce drastically different seismic response depending on whether they are truly unconsolidated or have initial quartz cementation.

III. **Data And Method**

Study Dataset

The dataset used in this study comprises a 3D post-stack seismic volume, migrated near- and far-offset partial stacks, and wireline log data acquired from the Paleogene succession of the northern North Sea. The dataset was obtained from the open repository described by Avseth et al. (2005).

Five exploration wells (Wells 1–5) were available, although only Wells 2 and 3 are located within the seismic sub-volume used for inversion. The available well logs include P-wave sonic, bulk density, gamma-ray, neutron porosity, and shear-wave logs. Density and compressional sonic logs were available in all wells, while gamma-ray and neutron porosity logs were present in Wells 1–4. Shear-wave velocity data were available only for Wells 2 and 5. Corrected density logs and lithofacies information for Well 2 were also provided for calibration and validation.

The seismic dataset consists of migrated 3D near- and far-offset partial-stack volumes in SEG-Y format. The survey was processed for true-amplitude preservation with a maximum fold of 30 and maximum source-receiver offset of approximately 2500 m. The analysis focused on a seismic sub-volume bounded by inlines 1300–1500, crosslines 1500–2000, and a two-way travel time window of 1500–2500 ms.

Data Preparation

Well logs were imported into Hampson-Russell GeoView for quality assessment and editing. Spurious measurements, spikes, and anomalous values in the density and sonic logs were removed prior to inversion. Edited logs were subsequently exported for inversion analysis.

Because sonic logs are recorded at ultrasonic frequencies that differ significantly from seismic frequencies, well-to-seismic calibration was performed to improve the correlation between synthetic and recorded seismic traces. This calibration minimized time-depth mismatches and enhanced the reliability of the inversion results.

The seismic volume was imported into Hampson-Russell STRATA, where density and compressional velocity logs were positioned at their respective well locations. Three regional seismic horizons, comprising the top Heimdal Formation, base Heimdal Formation, and an intermediate reference horizon, were manually interpreted to constrain the low-frequency impedance model.

Depth zones containing data for six different lithofacies identified in well 2 have been extracted and provided in separate text files. A corrected density log for well 2 is also provided

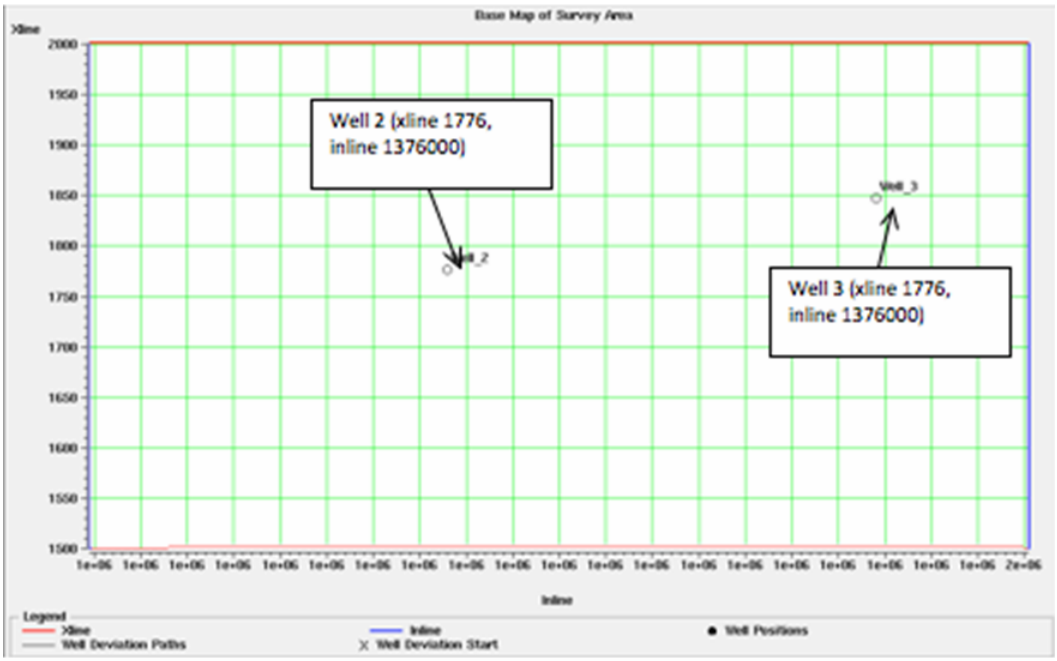

Figure 3. Approximate well locations within the 3D sub-cube. Absolute locations are unknown.

Acoustic Impedance Inversion

Model-based post-stack acoustic impedance inversion was employed to transform band-limited seismic reflection amplitudes into absolute acoustic impedance values. The inversion integrates seismic reflection data with low-frequency impedance information derived from well logs to generate a broadband impedance model of the Heimdal Formation.

Acoustic impedance (AI) was calculated as: $AI = \rho \times V_p$ 1

where ρ is rock density and Vp is compressional-wave velocity.

Prior to inversion, a statistical wavelet was extracted from the seismic data. Several extraction parameters were evaluated through well-to-seismic tie analysis. The optimum wavelet consisted of a 150 ms wavelet length, 20 ms taper length, and 320 ms extraction window, providing the highest correlation between synthetic and observed seismic traces.

The inversion workflow consisted of the following stages:
- Importation of seismic and well-log datasets;
- Well-log editing and quality control;
- Horizon interpretation;
- Well-to-seismic calibration;
- Statistical wavelet extraction;
- Construction of the low-frequency impedance model;
- Model-based acoustic impedance inversion;
- Quality assessment using residual analysis.

Velocity and Porosity Prediction

The inverted acoustic impedance volume was further transformed into P-wave velocity and porosity volumes using empirical relationships implemented in Hampson-Russell EMERGE.

Velocity was estimated from the impedance model through least-squares regression between impedance and measured sonic velocity obtained from the calibration wells. Porosity was estimated using the established inverse relationship between acoustic impedance and reservoir porosity, calibrated with available well-log measurements. These transformations enabled quantitative evaluation of reservoir quality and lateral variations in the Heimdal Formation across the study area.

Validation of Inversion Results

The reliability of the inversion was evaluated by comparing predicted acoustic impedance and porosity with corresponding well-log measurements at calibration wells. Correlation coefficients obtained from the well-to-seismic ties and impedance-porosity relationships were used to assess inversion accuracy.

The validated acoustic impedance, velocity, and porosity volumes were subsequently interpreted to characterize lithological variability, reservoir continuity, and lateral heterogeneity within the Paleogene Heimdal Formation.

IV. **Results**

Data Processing

The post-stack seismic inversion workflow was implemented using Hampson-Russell STRATA, while well-log management and editing were performed in GEOVIEW and eLOG. Prior to inversion, the density and P-wave sonic logs were carefully quality-controlled by removing spikes and anomalous measurements to improve the reliability of the impedance model. The corrected logs were subsequently imported into GEOVIEW for integration with the seismic data. (Figure 4)

The migrated 3D seismic volume was imported in SEGY format. Because acquisition and processing datum information was unavailable, the seismic data were referenced to a zero-millisecond datum. Well locations were correctly positioned within the seismic cube to facilitate well-to-seismic calibration (Figure 5).

Three key stratigraphic horizons, namely the Top Heimdal, Base Heimdal, and an additional regional marker horizon, were manually interpreted throughout the seismic volume. These horizons provided essential structural constraints during low-frequency model construction and ensured geological consistency during acoustic impedance inversion.

To tie the well to the seismic data, synthetic seismogram has to be generated. This is a form of 1-D forward model, which is expressed as the convolution of the source signature with the earth's impulse response. This is illustrated mathematically below:

$$S(t) = w(t) * e(t) + n(t) \qquad 2$$

Where $S(t)$ is the synthetic seismogram

$w(t)$ is the basic seismic wavelet

$e(t)$ is the earths impulse response

$n(t)$ is random ambient noise

Wavelet estimation was carried out using the statistical wavelet extraction algorithm available in STRATA. Several combinations of wavelet length, extraction window, and taper length were tested to optimise the well-to-seismic tie. The optimum solution was achieved using a 150 ms wavelet length, 320 ms extraction window, and 20 ms taper length. The resulting synthetic seismograms produced correlation coefficients of 0.58 for Well 2 and 0.49 for Well 3, indicating acceptable agreement between the seismic traces and the well data (Figure 6).

Acoustic Impedance Inversion

Sparse-spike acoustic impedance inversion was performed using the calibrated wavelet and the low-frequency impedance model generated from the available wells. Since only Wells 2 and 3 were located within the 3D seismic sub-volume, the inversion relied primarily on these wells to constrain the low-frequency impedance trends.

The inversion successfully transformed the band-limited seismic amplitudes into quantitative acoustic impedance values, thereby improving vertical resolution and enabling more reliable lithological interpretation. The generated acoustic impedance volume formed the basis for subsequent velocity and porosity estimation.

Velocity and Porosity Prediction

Velocity and porosity models were generated from the inverted acoustic impedance volume using empirical rock-physics relationships implemented in EMERGE. The velocity model was derived through least-squares regression between acoustic impedance and measured P-wave velocity, whereas porosity estimation employed the Wyllie time-average equation.

Inversion Processes

As stated in section III, the data available for this project consists of 251 cross lines and 101 inlines. Out of the five wells only two are within the 3D sub-cube, hence other wells could not be used as input the seismic inversion. The problem of having few wells in the inversion process is that, if a survey area has only a few wells from which to derive the low frequencies required for prior model generation, there may be variance away from the well that will not be captured by the low frequency model.

Due to loss of high frequency in the seismic process, the information required to reconstruct the velocity profile is not present in the seismic data. This implies that the seismic data is bandlimited, therefore the need to increase the bandwidth of the input model into the inversion process. The bandwidth of the initial model is increased by adding the low frequency content (which is assumed to be missing in the seismic data) from the wells hence improve the resolution of the inverted volume.

The initial model represents an initial guess at the velocity structure used in constraining the inversion. The final result being a velocity profile that deviates as little as possible from the initial model while at the same time modelling the real data as closely as possible (STRATA manual)

- Derived velocity section

In EMERGE, the velocity is calculated using the generalised equation (3) below.

$V = aI^{\wedge}b$ 3

where V = Velocity

I = Impedance

a and b are determined by least squares fitting of the velocity and impedance from the initial guess model.

- Porosity transform section

This section is derived in EMERGE by using Wyllie's equation shown below. This assumed linear equation specifies a relationship between porosity and density:

$\emptyset = (dt - dt_{matrix})/(dt_{fluid} - dt_{matrix})$ 4

Where dt = transit time

dt_{matrix} = transit time for the rock matrix

dt_{fluid} = transit time of the interstitial fluids

The resulting property volumes revealed considerable spatial variability across the Heimdal Formation, reflecting lateral changes in reservoir quality and depositional architecture.

Interpretation of Inversion Results

The inverted acoustic impedance sections reveal significant heterogeneity within the Heimdal Formation. Acoustic impedance values generally range from approximately 2,000 to 5,700 m/s·g/cc, although localized zones exceed 6,200 m/s·g/cc, indicating relatively cemented sandstone intervals.

At Well 2, the inversion clearly delineates alternating sandstone and shale packages, with the sandstone units exhibiting relatively low acoustic impedance compared to the surrounding lithologies. These impedance contrasts correspond closely with the interpreted lithofacies and demonstrate the capability of sparse-spike inversion to resolve thin reservoir units.

The derived velocity sections further distinguish the principal lithofacies. Cemented sandstone exhibits the highest velocities (approximately 2,866–3,012 m/s), whereas unconsolidated clean sandstone displays intermediate velocities (2,720–2,866 m/s). Silty sandstone and silty shale occupy intermediate ranges, while shale units are characterized by comparatively lower velocities.

Porosity estimates generally range between 25% and 40%, indicating fair to excellent reservoir quality within the Heimdal Formation. Although local discrepancies exist between measured and predicted porosity, the inversion-derived porosity model reproduces the overall reservoir trend with a correlation coefficient of approximately 68%, confirming the reliability of the inversion approach.

Spatial analysis of the impedance, velocity, and porosity volumes demonstrates pronounced lateral variations throughout the study area. The reservoir sand bodies occur as discontinuous, sigmoidal geometries that are characteristic of deep-water turbidite channel systems. These geometries support the interpreted depositional model of channelized Paleocene submarine fan deposits.

Overall, the inversion results demonstrate that acoustic impedance inversion significantly improves the delineation of reservoir architecture beyond well control and provides reliable estimates of lateral variations in lithology, velocity, and porosity within the Heimdal Formation (Figure 7).

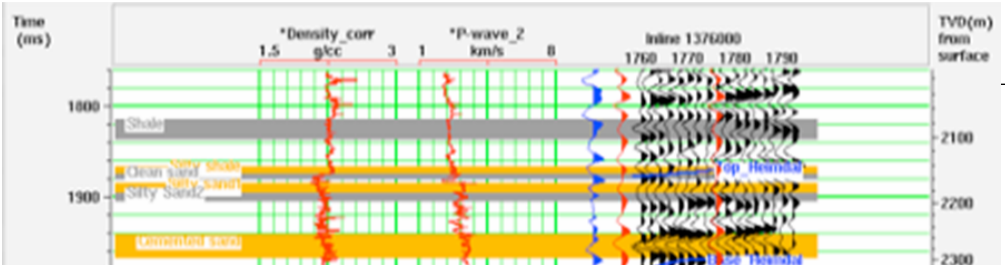

Figure 4. Well-to-seismic correlation at well 2 and estimated wavelet used in the acoustic impedance inversion. The final extracted wavelet and its frequency spectrum are also shown. Correlation factor of 0.58 *is for the entire well and is considered a good value as the tie focussed only on the horizons of interest.*

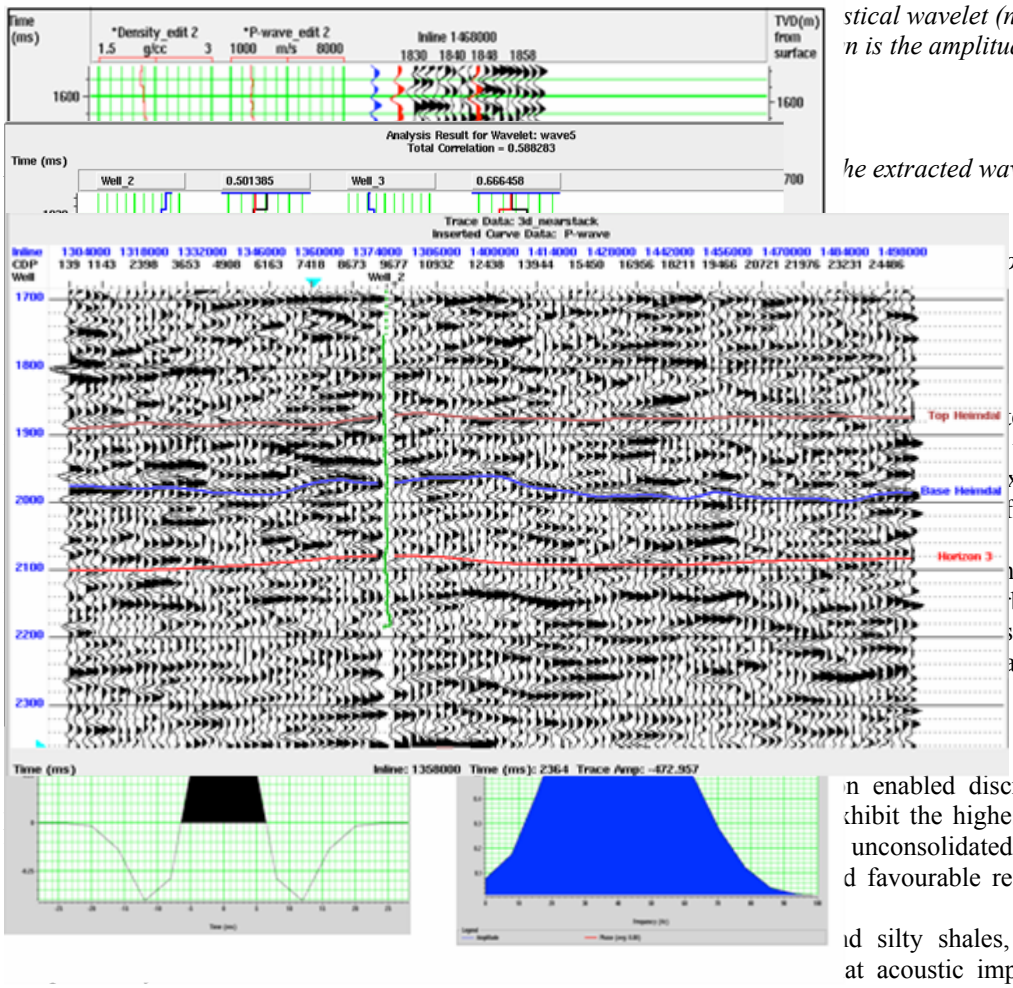

stical wavelet (normal polarity) n is the amplitude and frequency

he extracted wavelet with the well

ons extrapolated

eral and vertical that the reservoir ximately 3,800 to flect differences in

ibits pronounced bedded sandstone sistent with poorly are interpreted as

n enabled discrimination of the hibit the highest impedance and unconsolidated clean sandstones d favourable reservoir properties

d silty shales, while shale has at acoustic impedance inversion provides an effective means of differentiating lithological units that are difficult to resolve using conventional seismic amplitude interpretation alone.

Reservoir Property Variation

The derived velocity and porosity transforms indicate significant spatial variability in reservoir properties across the study area. Predicted porosity values generally range between 25% and 40%, suggesting that the Heimdal Formation possesses very good to excellent reservoir quality despite local heterogeneity (Figure 9 & 10).

Although the inverted porosity sections reproduce the overall reservoir trend observed in the well logs, minor discrepancies occur locally. These differences are likely attributable to lithological complexity, thin-bed interference, and the assumptions employed during impedance-to-porosity transformation. Nevertheless, the predicted porosity distribution agrees reasonably well with measured well-log porosity, confirming the reliability of the inversion workflow.

Lateral Reservoir Continuity

Interpretation of the inverted sections demonstrates that the Heimdal sandstones occur as laterally discontinuous, channelized sand bodies. Around Well 2, the reservoir displays a distinct sigmoidal geometry, characteristic of deep-water turbidite channel deposits (Figure 9). These discontinuous geometries indicate rapid lateral facies variations, which are typical of submarine fan depositional systems.

In contrast, the reservoir interval surrounding Well 3 exhibits weaker acoustic impedance contrast, making reservoir boundaries less distinct. This reduced contrast may reflect thinner sandstone development, lower impedance contrast between sand and shale, or variations in reservoir quality (Figure 10).

The inversion results consistently indicate that the Heimdal Formation comprises discrete sandstone bodies distributed throughout the three-dimensional seismic volume rather than a laterally continuous reservoir unit. Such heterogeneity has important implications for reservoir connectivity and hydrocarbon production strategies.

Implications for Reservoir Characterization

The inversion-derived acoustic impedance model significantly improves subsurface characterization beyond conventional seismic interpretation. The results demonstrate that acoustic impedance inversion can successfully identify lateral variations in lithology, estimate reservoir quality, and delineate channelized sandstone bodies within complex turbidite systems.

The relatively low impedance and high predicted porosity observed across much of the Heimdal Formation indicate favourable reservoir conditions. However, localized cementation and shale intercalations introduce significant heterogeneity that may influence fluid flow and reservoir performance. Consequently, integrating acoustic impedance inversion with petrophysical analysis provides a more robust framework for reservoir evaluation and reduces uncertainty in reservoir prediction.

Overall, the study confirms that sparse-spike acoustic impedance inversion is an effective tool for imaging thin, heterogeneous Paleogene turbidite reservoirs and for predicting reservoir properties away from existing well control.

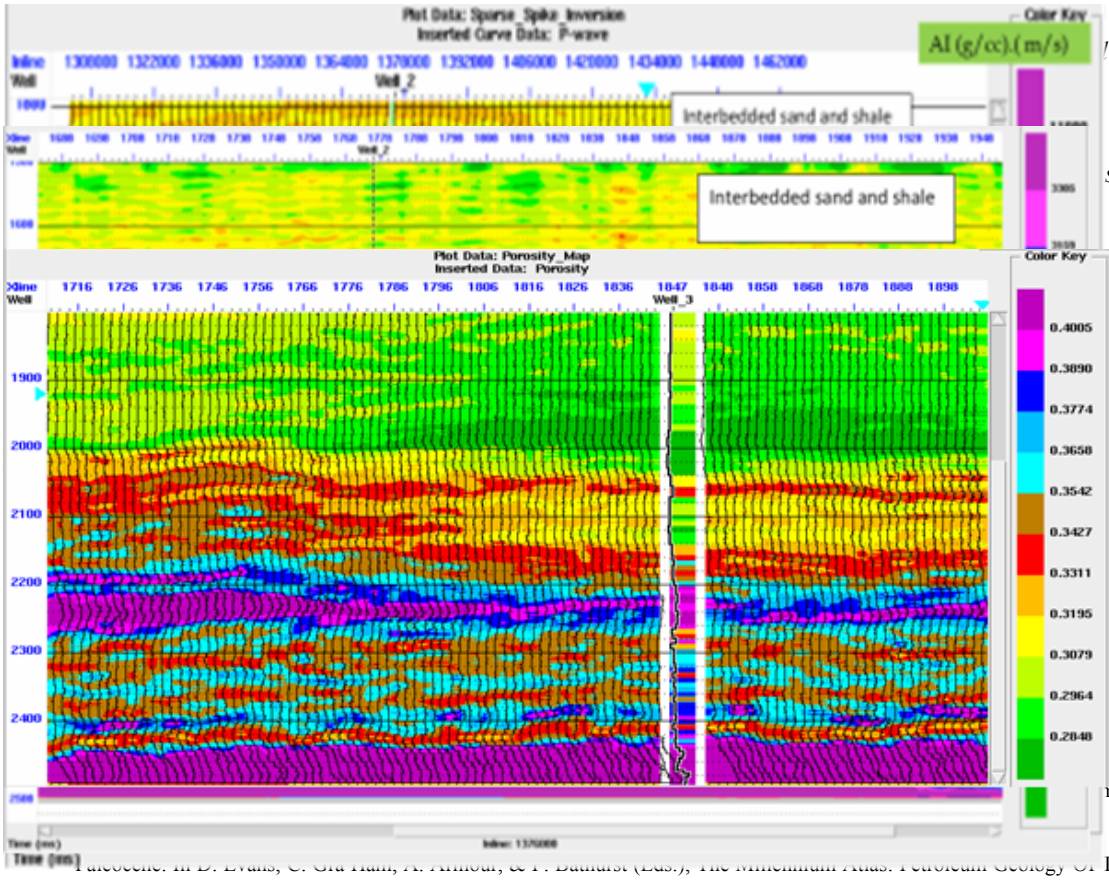

l scale is

scale is

le is the
ns' .

reservoir
onstrated
edict the
volume
ecture of
e spatial
tool for
ep-water

nic Genetic

G. (2003). The Central And Northern North Sea (Pp. 235–259). Geological Society Of London.

[3]. Alistair, R. B. (1992). Technologies In Reservoir Geophysics. In R. E. Sheriff (Ed.), Reservoir Geophysics. Society Of Exploration Geophysicists.

[4]. Avseth, P., Mukerji, T., Jørstad, A., Mavko, G., & Veggeland, T. (2001). Seismic Reservoir Mapping From 3-D Avo In A North Sea Turbidite System. Geophysics,

[5]. Avseth, P., Mukerji, T., Mavko, G., & Tyssekvam, J. A. (2000). Rock Physics And Avo Analysis For Lithofacies And Pore Fluid Prediction In A North Sea Oil Field. The Leading Edge, 20, 429–434.

[6]. Avseth, P., Flesche, H., Wijngaarden, A., & Mavko, G. (2003). Avo Classification Of Lithology And Pore Fluids Constrained By Rock Physics Depth Trends. The Leading Edge, 28, 1004–1011.

[7]. Avseth, P., Jørstad, A., Wijngaarden, A., & Mavko, G. (2005). Rock Physics Estimation Of Cement Volume, Sorting, And Net-To-Gross In North Sea Sandstones. The Leading Edge, 24, 98–108.

[8]. Eissa, M. A., Pfeiffer, J., & Ortega, A. P. (2009). Seismic Petrophysical Analysis For Thin Sandstone Reservoirs In Colombia's Guajira Basin. The Leading Edge, 28, 640–647.

[9]. Hampson-Russell Software. (1999). Strata/Unix Stratigraphic Analysis And Inversion Manual. Hampson-Russell Software.

[10]. Haq, B. U., Hardenbol, J., & Vail, P. R. (1988). Mesozoic And Cenozoic Chronostratigraphy And Cycles Of Relative Sea-Level Change. In C. K. Wilgus Et Al. (Eds.), Sea-Level Changes: An Integrated Approach (Pp. 72–101). Sepm Special Publication No. 42.
[11]. Jordt, H., Faleide, I. E., Bjørlykke, K., & Ibrahim, M. T. (1995). Cenozoic Sequence Stratigraphy Of The Central And Northern North Sea Basin: Tectonic Develop Ment, Sediment Distribution And Provenance Areas. Marine And Petroleum Geology, 12(8), 845–879.
[12]. Knox, R. W. O'b., & Holloway, S. (Eds.). (1992). Paleogene Of The Central And Northern North Sea: Lithostratigraphic Nomenclature Of The Uk North Sea (Vol. 1). British Geological Survey.
[13]. Neal, J. E. (1996). A Summary Of Paleogene Sequence Stratigraphy In Northwest Europe And The North Sea. In R. W. O'b. Knox, R. M. Corfield, & R. E. Dunay (Eds.), Correlation Of The Early Paleogene In Northwest Europe (Pp. 15–42). Geological Society Special Publication No. 101.
[14]. O'connor, S. J., & Walker, D. (1993). Paleocene Reservoirs Of The Everest Trend. In J. R. Parker (Ed.), Petroleum Geology Of Northwest Europe: Proceedings Of The 4th Conference (Pp. 141–160). Geological Society.
[15]. Tiekuro, E., Emujakporue, G. O., & Nwankwo, C. N. (2024). Application Of Post-Stack Acoustic Impedance Inversion To Lateral Rock Property Prediction: A Case Study Of Eti Field, Offshore Niger Delta. European Journal Of Science And Engineering, 67, 283–305.
[16]. Whyatt, J., Bowen, J. M., & Rhodes, D. N. (1991). Successful Application Of A Development Geoseismic Model In North Sea Exploration. Geological Society, London, Special Publications, 67, 283–305.
[17]. Yilmaz, O. (2001). Seismic Data Analysis: Processing, Inversion, And Interpretation Of Seismic Data (Vol. 2). Society Of Exploration Geophysicists.